An assessment of the accuracy of the RTTOV fast radiative transfer model using IASI data

Marco Matricardi, Tony McNally

ECMWF
Reading, Berkshire, UK

Abstract

IASI measurements of spectral radiances made the 1st April 2008 are compared with simulations performed using the RTTOV fast radiative transfer model utilizing regression coefficients based on different line-by-line models. The comparisons are performed within the framework of the European Centre for Medium-Range Weather Forecasts Integrated Forecasting System using fields of temperature, water vapour and ozone obtained from very short range forecasts. Simulations are performed in controlled conditions to study the behaviour of the different line-by-line models and spectroscopic parameters on which the RTTOV coefficients are based.

Introduction

The exploitation of satellite radiance data for numerical weather prediction (NWP) requires the use of a fast radiative transfer (RT) model to simulate radiances from an input atmospheric profile. The variational approach to the assimilation of data into a NWP system involves the definition of the observation-error covariance matrix that is used to specify errors associated with radiance data. The observation-error covariance matrix is the sum of the instrumental-error covariance matrix and the forward-model-error covariance matrix which is based on the estimation of errors associated with fast RT models. RT errors are therefore an important consideration in the definition of the observation-error covariance matrix and consequently must be properly evaluated and fully understood.

The fast RT model used operationally at ECMWF is the Radiative transfer model for TOVS (RTTOV) (Matricardi et al. 2004). RTTOV is a regression based fast RT model on fixed pressure levels. It can be used in conjunction with a number of regression coefficients generated using different line-by-line (LBL) models. Regression coefficients for IASI are available based on the GENLN2 (Edwards 1994), LBLRTM (Clough et al.1992) and kCARTA (Strow et al. 1998) LBL models. In this paper we study the accuracy of the RTTOV computations by running four Integrated Forecast System (IFS) monitoring experiments where we compare the simulated spectra with spectra measured by IASI during the 1st April 2008. Results presented in this paper are very preliminary since spectra could only be processed over a limited time period due to the late implementation of the latest version of RTTOV into the Integrated Forecastin System (IFS).

The monitoring experiments

Four monitoring experiments have been run using cycle 33R1 of the IFS at the T799 full horizontal resolution (~25 km). A feature of cycle 33R1 is a vertical discretization of the atmosphere into a grid of 91 pressure levels. The spacing of the grid follows the horography of the terrain while the top level is fixed at 0.01 hPa. The state vector variables used in the RTTOV simulations are forecast fields of temperature, humidity and ozone. IASI data within a 12-hour 4D-VAR window are grouped into 30 minutes time slots. A T799 high resolution forecast is then run every 30 minutes from the previous analysis and observation minus model differences are computed for IASI soundings that, within a time slot, fall inside a 15 minute interval either side of the forecast time. This sequence is

then repeated for each 12-hour 4D-VAR window. In this study we consider IASI data inside two 4D-VAR windows on the 1st April 2008.

Each monitoring experiment is based on a different RTTOV coefficient file as shown in Table1.

Table 1: the regression coefficients used for the RTTOV simulations

Coefficients	Continuum	CO_2 line mixing	Molecular database
Line-by-line model: kCARTA *Number of vertical levels:* 43 *Training set:* 52 profile training set	MTK_CKD_v1.1_UMBC	P/Q/R branch (υ2 and υ3 band)	HITRAN_2000
Line-by-line model: GENLN2 *Number of vertical levels:* 43 *Training set:* 43 profile training set	CKD_2.1	Q branch (υ2 and υ3 band)	HITRAN_1996
Line-by-line model: GENLN2 *Number of vertical levels:* 100 *Training set:* 43 profile training set	CKD_2.4	Q branch (υ2 and υ3 band)	HITRAN_2000
Line-by-line model: LBLRTM *Number of vertical levels:* 100 *Training set:* 83 profile training set	MTK_CKD_v1.1	P/Q/R branch, υ2, υ3 band	HITRAN_2000 HITRAN_2004/06 GEISA_2003

From Table 1 it can be seen that the regression coefficients have been generated using the kCARTA, GENLN2 and LBLRTM LBL models. Important differences also exit between the water vapour continuum model, the CO_2 line mixing model and the molecular database used in each LBL computation. Table 1 also shows that regression coefficients are generated using various profile training sets and for different numbers of vertical pressure levels. Regarding the pressure levels, it should be noted that although RTTOV computes optical depths on the levels specified in the coefficient files, the integration of the RT equation is performed on the 91 IFS levels using the internal interpolation routine implemented in the latest version of RTTOV. Note how the GENLN2 model includes the effects of CO2 line coupling only for the CO2 Q branches (Strow et al. 1994) whereas kCARTA and LBLRTM include the effects of line mixing also for the P and R branches using the models by Strow et al. (2003) and Niro et al. (2005) respectively. The self- and foreign-broadened water vapour continuum absorption is included in all computations using different versions of the CKD and MTK_CKD model (Clough et al. 1989). In particular, kCARTA features a revised version on the MTK_CKD model based on the use of AIRS clear sky data and radiosondes at the ARM sites (Machado 2008). Figures 1 and 2 show the water vapour broadening coefficients for some of the models used in this study (self broadening is the dominant source of continuum in the window regions whereas foreign broadening dominates in the water vapour band) As Figure 1 shows, in the 10 μm window region MTK_CKD_UMBC self broadening coefficients are smaller than CKD_2.4 and MTK_CKD_v1.1 coefficients. In the centre of the water vapour band around 1600 cm-1 the CKD_2.4 foreign broadening coefficients are smaller that MTK_CKD_UMBC and MTK_CKD_v1.1

coefficients whereas for larger wave numbers MTK_CKD_UMBC foreign broadening coefficients are larger than CKD_2.4 and MTK_CKD_v1.1 coefficients (Figure 2).

Finally, note how for the LBLRTM computations we use molecular database that is the blend of molecular parameters from HITRAN_2000 (Rothman et. al 2003), HITRAN_2004/06 (Rothman et. al 2005) and GEISA_2003 (Husson ert al. 2005)

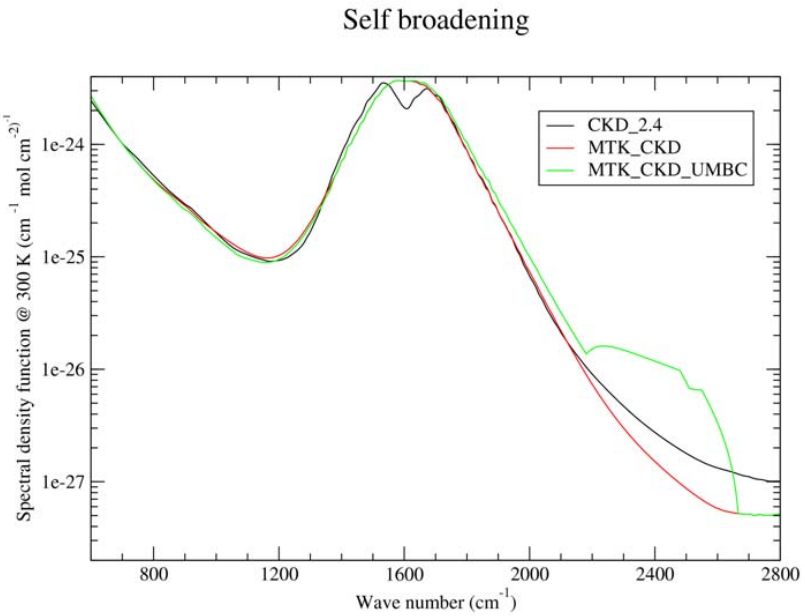

Figure 1: spectral density function for the water vapour self broadening coefficients at 300K and 1013 hPa.

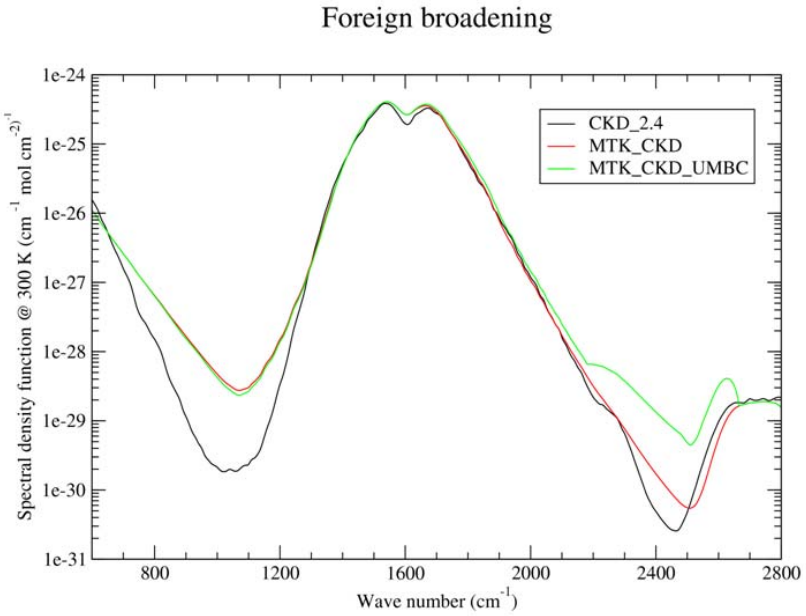

Figure 2: spectral density function for the water vapour foreign broadening coefficients at 300K and 1013 hPa.

The IASI spectra used in our experiments are measured over the sea and only channels detected as clear by the ECMWF cloud detection algorithm are processed. Since the ECMWF cloud detection algorithm (McNally and Watts 2003) finds clear channels rather than clear locations, the size of sample varies with the sensitivity of the channel to surface emitted radiance: i.e. channels characterized by weighting functions that peak at high altitudes are less sensitive to clouds than channels with weighting functions that peak at low altitudes or at surface. To illustrate this we show in Figures 3 and 4 the number of clear radiances for a surface channels and for a stratospheric channels respectively. It can be clearly seen that the number of clear radiances detected for the stratospheric channels outnumber by far the clear radiances detected for the surface channel.

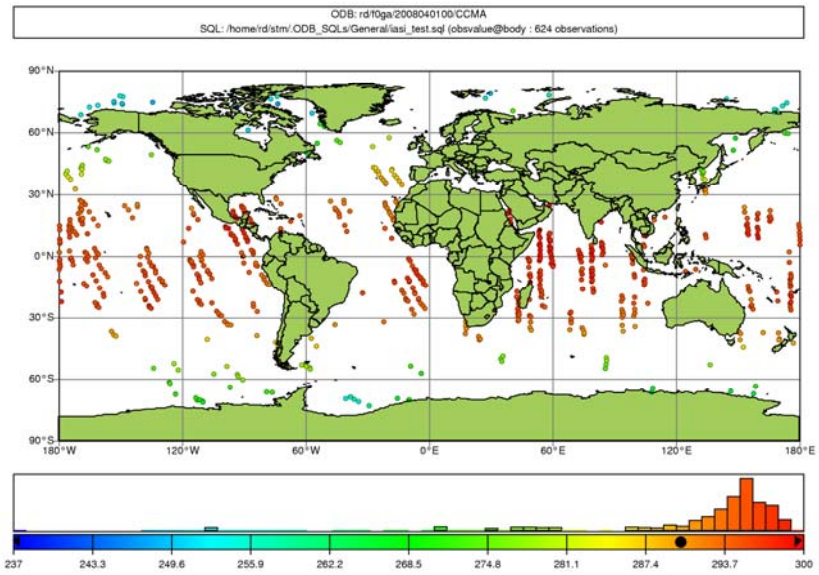

Figure 3: the clear radiances detected for a surface channel.

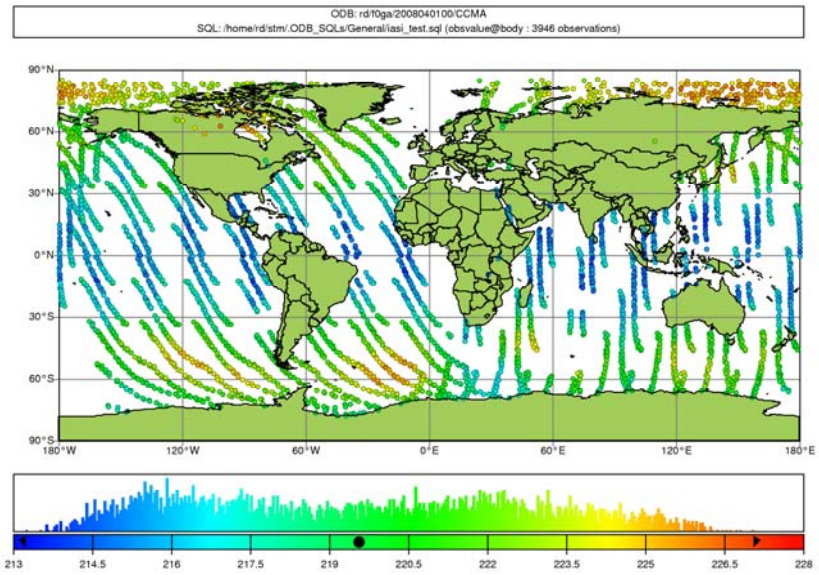

Figure 4: the clear radiances detected for a stratospheric channel.

The size of the sample for each channel is shown in Figure 5 for the tropical latitude band (30ºS - 30º N). It can be clearly seen that the size of the sample amount to thousands of spectra for the channels peaking at middle and high altitudes whereas the sample for channels peaking at low altitudes or at surface amounts to hundreds of spectra.

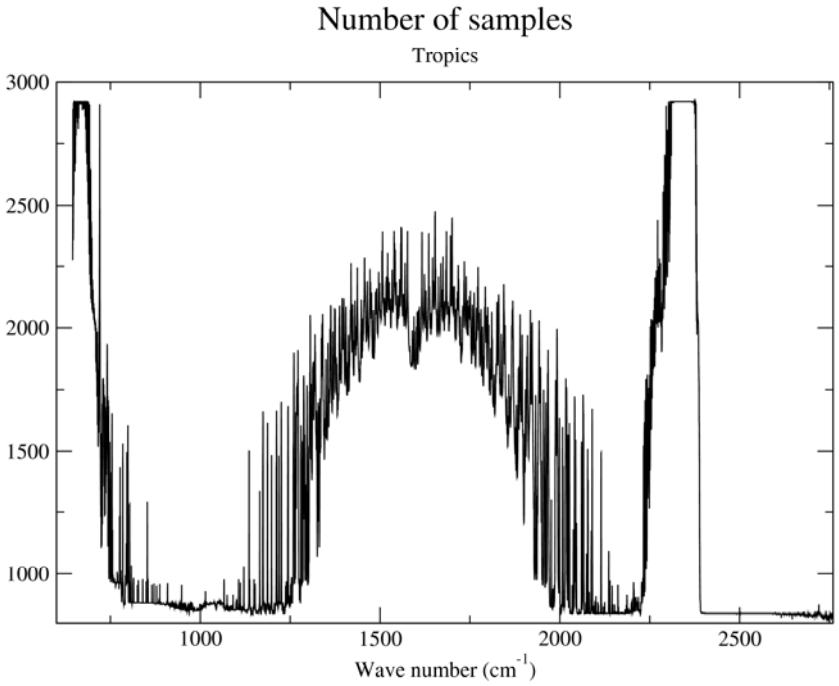

Figure 5: the size of the sample for the tropical latitude band.

In our RTTOV computations the state vector includes profiles of temperature, water vapour and ozone, surface parameters (e.g. skin temperature and surface pressure) and a wave number dependent value of the sea surface emissivity that includes the dependence on the viewing geometry. In addition to the profiles of temperature, water vapour and ozone, the experiments that use RTTOV coefficients on 100 vertical levels also require input profiles of CO_2, CO, N_2O and CH_4. This is not the case for the 43 level coefficients where constant climatological values are assumed in the LBL computations used to train the fast model. Since profiles for trace gases are not prognostic variables in the ECMWF model we had to fix the trace gas profiles in the 100 level experiments. To this end we have chosen the values assumed in the LBL computation used to train kCARTA. The rationale behind this choice is that at present kCARTA coefficients are used operationally at ECMWF and we want to use the kCARTA spectra as benchmark in our comparisons.

Results

In Figure 6 we show the mean value of the difference (bias) in units of brightness temperature for the latitude band between 30º N and 90º N. The top panel show results for the GENLN2 and kCARTA 43 level experiments (henceforth GENLN2_43 and kCARTA_43) whereas in the middle and bottom panel the GENLN2 and LBLRTM 100 level experiments (henceforth GENLN2_100 and LBLRTM_100) are superimposed to the kCARTA_43 experiment. Note how results are only shown for IASI band 1 and 2. At the time the experiments were carried out we were not sure about the correct implementation into the IFS

of the 100 level regression coefficients in IASI band 3 and consequently have decided not to show the results for this band until the issue is fully resolved.

Figure 6 shows that for all experiments biases are generally below 1 K in all spectral regions. The only exception is the ozone band at 9.8 μm where biases are consistently larger that 1 K probably reflecting some intrinsic weakness of the ozone assimilation system. Of particular interest are the result in 15 μm temperature sounding region. It can be clearly seen that all the experiments based on GENLN2 show larger biases between 700 cm^{-1} and 750 cm^{-1}. We attribute this feature to the fact that GENLN2 does not feature CO_2 P/R branch line mixing in this region. For the experiments that feature CO2 P/R branch line mixing (kCARTA_43 and LBLRTM_100) biases are within 0.5 K and between 645 cm^{-1} and 720 cm^{-1} the experiments on 101 levels exhibits biases that are remarkably below 0.2 K. In the window region the GENLN2_43 experiment shows larger biases probably due to the use of an early version of the water continuum model. Al the experiments give very similar results between 900 cm^{-1} and 1200 cm^{-1}. Most of the differences between kCARTA_43 and GENLN2_43 in the CH_4 band (top panel, 1200 cm^{-1} - 1400 cm^{-1} region) can be attributed to the fact that the concentration used in the underlying LBL computations is different (and cannot be changed). It should also be noted that some of the differences in this spectral region can be attributed to the water vapour molecular parameters used in GENLN2_43. As discussed previously, the CH_4 concentration can be changed in the 100 level experiments and we have fixed it to the value assumed in kCARTA. This is reflected in the middle and bottom panel where GENLN2_100 and LBLRTM_100 biases are much closer to kCARTA_43 biases. It should be noted however that since the CH_4 variability is not reflected in the RTTOV computations, a portion of the bias seen in all the experiments the CH_4 band can be attributed to this factor. An interesting feature of Figure 6 is the behaviour of GENLN2 around 1600 cm^{-1}. The larger biases seen for the GENLN2 experiments around this wave number reflect, in our opinion, the difference between the water vapour continua models. In other regions of the water vapour band differences are not so obvious to interpret. The fact that the GENLN2_43 and kCARTA_43 spectra shown in the top panel are in good agreement (note how the two experiments use different molecular databases) hints to the fact that differences seen in the middle and bottom panel can be partially attributed to the number of levels on which the regression coefficients are provided although the impact of differences between water vapour continuum models cannot be completely ruled out.

Standard deviations are shown in Figure 7. They are comparable to biases in the window regions and in the temperature sounding region whereas they tend to be larger than biases in the ozone sounding region and in the water vapour band. Some larger values of the standard deviation in the water vapour band can be attributed to the instrument noise as well as in the region between 645 cm^{-1} and 670 cm^{-1}.

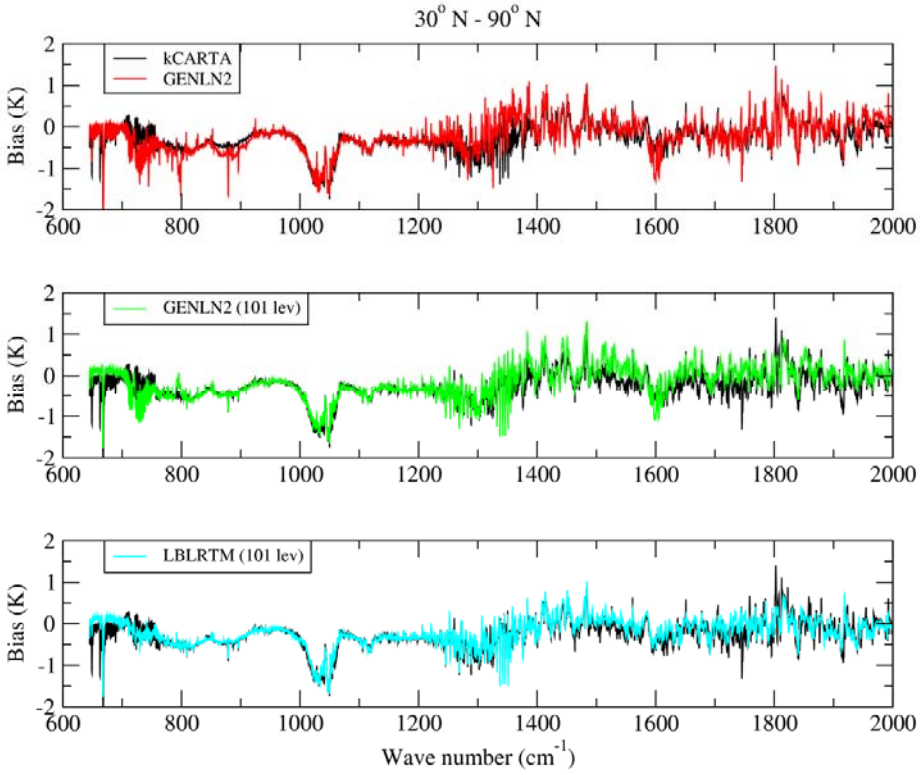

Figure 6: the mean value of the difference between observed and computed brightness temperatures for the northern hemisphere.

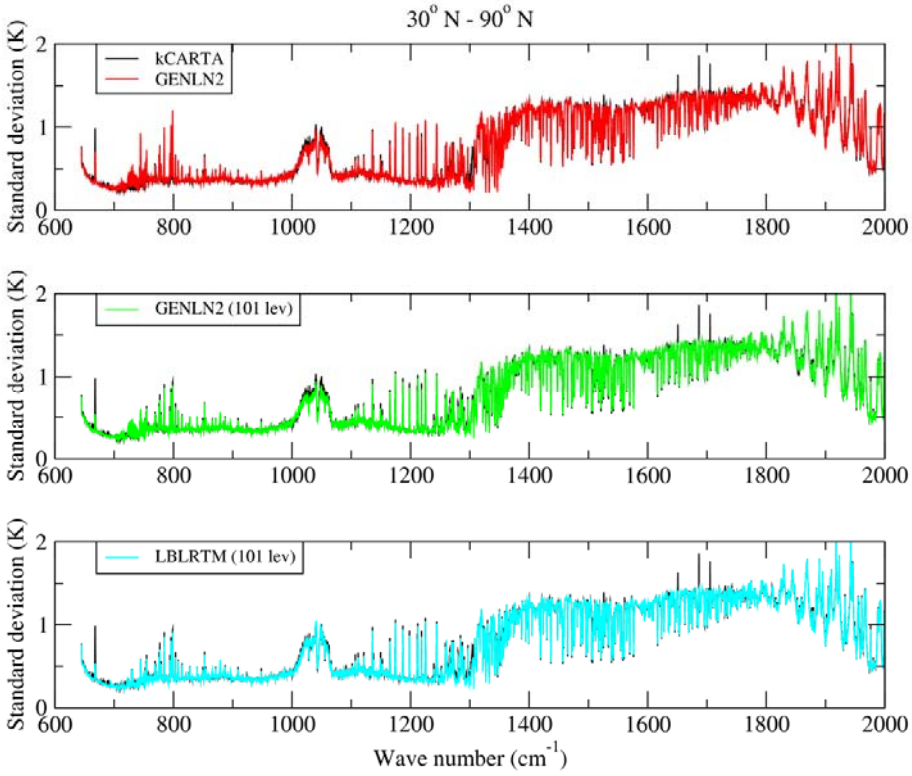

Figure 7: the standard deviation of the difference between observed and computed brightness temperatures for the northern hemisphere.

Results for the tropical band (30º S - 30º N) are shown in Figures 8 and 9. It is evident how biased have increased above all in the regions dominated by water vapour absorption although in most of the spectral regions biases are still within ± 1K. Biases in the ozone sounding band are smaller that biases observed in the northern hemisphere and biases in the 15 μm sounding region are now within ±0.5 K compared to ±0.2 K observed in the northern hemisphere. CO_2 P/R branch line mixing still has a very significant impact on the spectra and improvements in the water vapour molecular parameters are very evident when the GENLN2_43 biases between 750 cm^{-1} and 1350 cm^{-1} are compared to the GENLN2_100, kCARTA_43 and LBLRTM_100 biases: i.e. the conspicuous absence of spikes in the latter experiments. The comparison between the GENLN2_100 and LBLRTM_100 experiments also provides, in our view, some evidence of the fact that results are clearly influenced by the water vapour continuum model. Noticeable in Figure 9 is the increase of the standard deviation in the water vapour band.

Finally, results for the southern hemisphere (30º S to 90º S) are shown in Figures 10 and 11. It is evident how biases have significantly decreased above all in the water vapour band. In general, conclusions drawn for the northern hemisphere can be applied to southern hemisphere as well with the exception of the fact that although biases in the water vapour band have decreased the maxim value of the standard deviation has actually increased and for a large number of channels values are comparable to those observed in the tropics. Most likely this is the combination of an increased instrument noise resulting from lower scene temperatures and a less robust assimilation of water vapour radiances in this hemisphere.

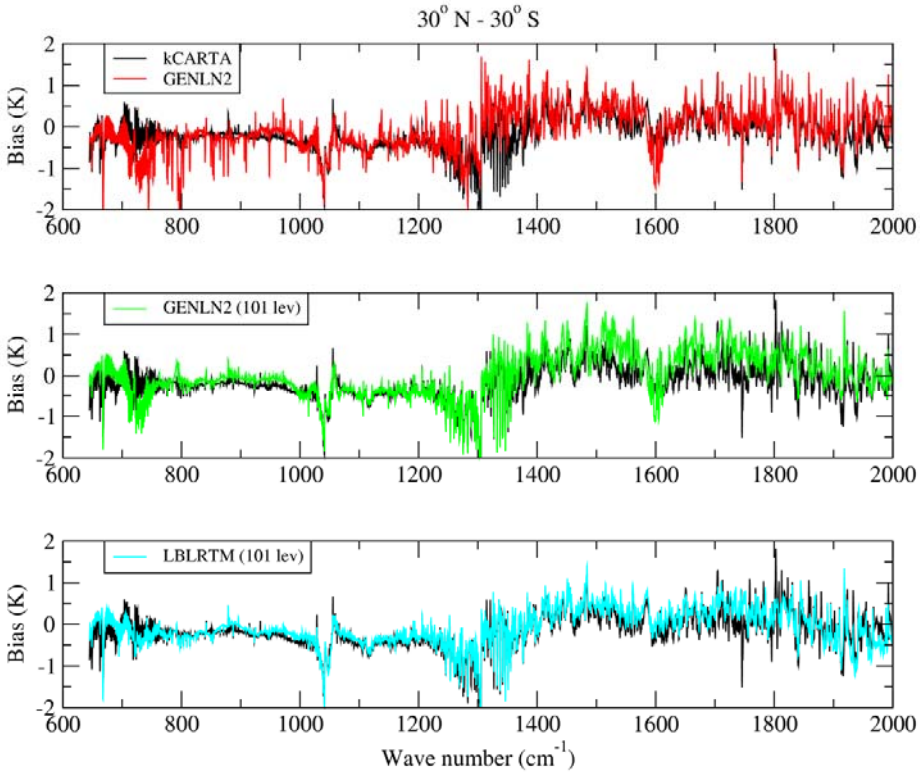

Figure 8: the mean value of the difference between observed and computed brightness temperatures for the tropics.

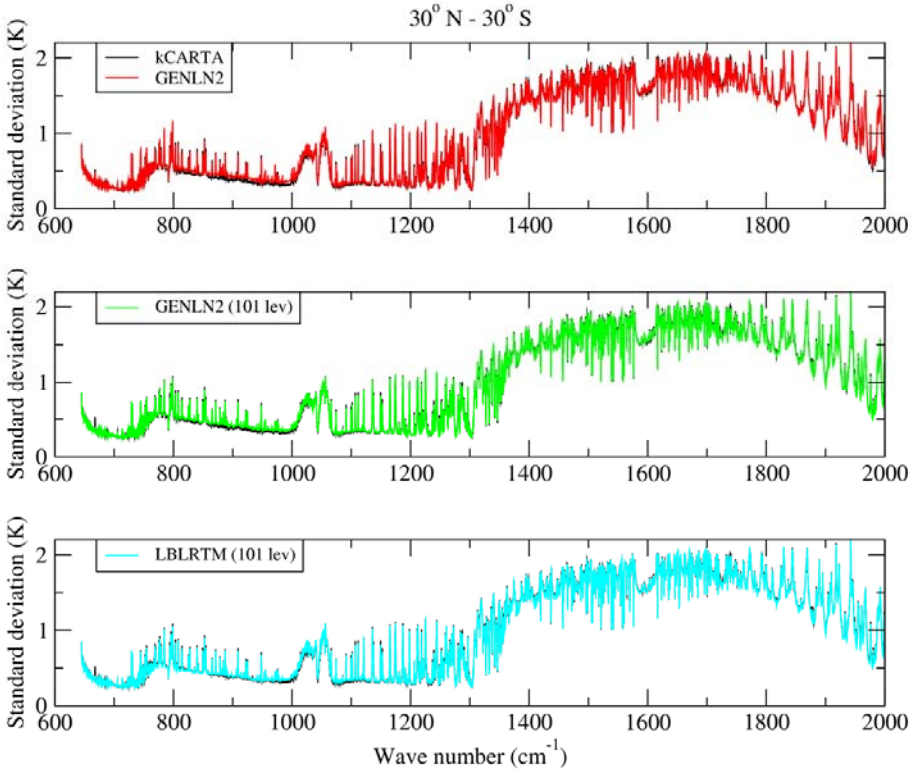

Figure 9: the standard deviation of the difference between observed and computed brightness temperatures for the tropics.

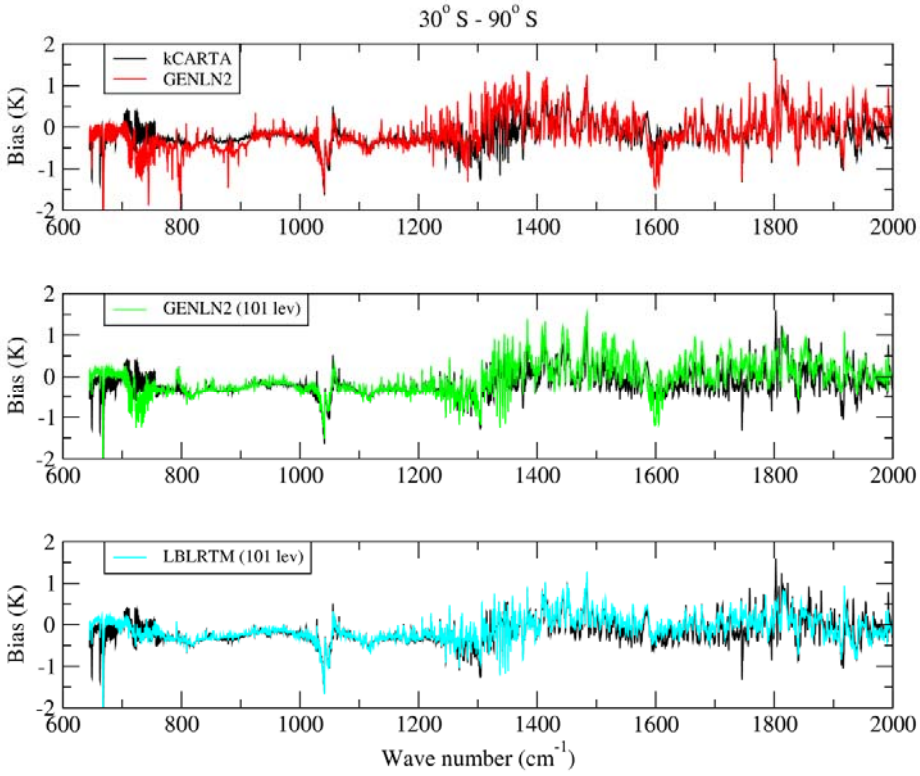

Figure 10: the mean value of the difference between observed and computed brightness temperatures for the southern hemisphere.

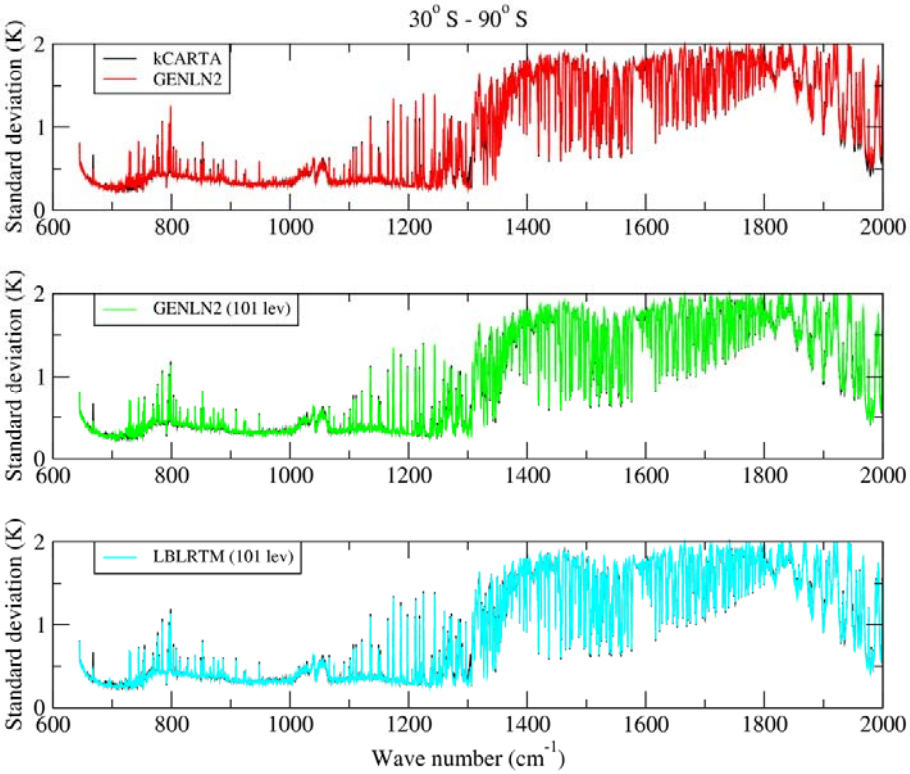

Figure 11: the standard deviation of the difference between observed and computed brightness temperatures for the southern hemisphere.

Conclusions

Four monitoring experiments have been run to compare IASI observed radiances to radiances simulated using the RTTOV fast radiative transfer model using regression coefficients based on different LBL models and molecular parameters. Results obtained for the 1st April 2008 using spectra over the sea and selecting clear channels (i.e. channels not affected by clouds) show that in the northern hemisphere biases are typically within ±1K. This figure is only exceeded in the ozone sounding band. CO_2 P/R branch line mixing has a significant impact on the simulated radiances resulting in a reduction of the biases up to 1K. In the water vapour band the use of the latest version of the water vapour continuum model results in a reduction of the bias of typically 1K in the region around 1600 cm^{-1}. The use of regression coefficients computed on a different number of pressure levels has an impact on the biases as well as the use of different water vapour continuum models. Biases in the tropics are typically larger than biases in the northern hemisphere although this is not the case in the ozone band where smaller biases are observed. However, in general, biases are still within ±1K in most of the spectral regions. The inclusion of CO_2 P/R branch line mixing is still effective in significantly reduce biases between 700 cm^{-1} and 750 cm^{-1} and there is evidence that the use of the latest version of the water vapour continuum model results in smaller biases. It should be noted however that these are very preliminary results. For practical and operational reasons the experiment were run over a very limited time period and the conclusions drawn in this paper could be affected by the availability of a larger sample of spectra. For this reason we are planning to run a further number of experiments over a much longer time period to accumulate a more robust statistics. Within this framework we want include experiments with kCARTA coefficients on 100 levels and a specification of the atmospheric state that reflects more realistically the concentration of the CO_2, CO, N_2O and CH_4 trace gas species.

Acknowledgements

We want to thank P. Brunel (Météo France) for having prepared the kCARTA coefficients.

References

Matricardi, M., F. Chevallier, G. Kelly and J.-N. Thepaut, 2004: "An improved general fast radiative transfer model for the assimilation of radiance observations". Q. J. Roy. Meteorol. Soc., **130**, 153-173.

Clough, S.A., F.X. Kneizys and R.W. Davis, 1989: Line shape and the water vapour continuum. *Atmospheric Research,* **23**, 229-241.

Clough, S.A, M.J., Iacono and J.-L., Moncet, 1992: Line by line calculation of atmospheric fluxes and cooling rates: application to water vapor. *J. Geophys. Res.*, **98**, pp. 15761-15785.

De Souza-Machado, S., personal comunication, 2008.

Edwards, D.P., 1992: GENLN2. A general Line-by-Line Atmospheric Transmittance and Radiance Model, NCAR Technical note NCAR/TN-367+STR, National Center for Atmospheric Research, Boulder,Co.

Jacquinet-Husson, N., N.A. Scott, A. Chedin, K. Garceran, R. Armante,A.A. Chursin, A. Barbe, M. Birk, L.R. Brown, C. Camy-Peyret, C. Claveau,C. Clerbaux, P.F. Coheur, V. Dana, L. Daumont, M.R. Debacker-Barilly,J.M. Flaud, A. Goldman, A. Hamdouni, M. Hess, D. Jacquemart, P. Kopke,J.Y. Mandin, S. Massie, S. Mikhailenko, V. Nemtchinov, A. Nikitin,D. Newnham,A. Perrin, V.I. Perevalov, L. Regalia-Jarlot, A. Rublev,F. Schreier, I. Schult, K.M. Smith, S.A. Tashkun, J.L. Teffo, R.A. Toth,Vl.G. Tyuterev, J. Vander Auwera, P. Varanasi, G. Wagner, 2005: The 2003 edition of the GEISA/IASI spectroscopic database. *J. Quant. Spectrosc. Radiat. Transfer*, **95**, 429-467.

McNally, A.P. and P.D. Watts, 2003. A cloud detection algorithm for high-spectral-resolution infrared sounders, Q J Roy Meteorol Soc, 129, 3411-3423.

Matricardi, M., F. Chevallier, G. Kelly and J.-N. Thepaut, 2004: "An improved general fast radiative transfer model for the assimilation of radiance observations". Q. J. Roy. Meteorol. Soc., **130**, 153-173.

Niro, F., K. Jucks and J.-M. Hartmann, 2005: Spectra calculations in central and wing regions of CO2 IR bands. IV: software and database for the computation of atmospheric spectra. Journal of Quantitative Spectroscopy and Radiative Transfer, Volume 95, Issue 4, Pages 469-481

Rothman, L.S., A. Barbe, D. Chris Benner, L.R. Brown, C. Camy-Peyret,M.R. Carleer , K. Chance, C. Clerbaux , V. Dana, V.M. Devi, A. Fayt,J.-M. Flaud, R.R. Gamache, A. Goldman, D. Jacquemart, K.W. Jucks,W.J. Lafferty, J.-Y. Mandin, S.T. Massie, V. Nemtchinov, D.A. Newnham,A. Perrin, C.P. Rinsland, J. Schroeder, K.M. Smith, M.A.H. Smith, K. Tang,R.A. Toth, J. Vander Auwera , P. Varanasi, K. Yoshino, 2003: The HITRAN molecular spectroscopic database: edition of 2000 including updates through 2001. *J. Quant. Spectrosc. Radiat. Transfer*, **82,** pp.5-44.

Rothman, L.S., D. Jacquemart,A. Barbe, D. Chris Benner, M. Birk,L.R. Brown, M.R. Carleer, C. Chackerian Jr., K. Chance, L.H. Coudert,V. Dana, V.M. Devi, J.-M. Flaud, R.R. Gamache, A. Goldman,J.-M. Hartmann, K.W. Jucks, A.G. Maki, J.-Y. Mandin, S.T. Massie,J. Orphal,2, A. Perrin,2, C.P. Rinsland, M.A.H. Smith, J. Tennyson,R.N. Tolchenov, R.A. Toth, J. Vander Auwera, P. Varanasi, G. Wagner, 2005: The HITRAN 2004 molecular spectroscopic database. *J. Quant. Spectrosc. Radiat. Transfer*, **96,** pp.139-204.

Strow, L. L., H. E. Motteler, R. G. Benson, S. E. Hannon, and S. De Souza-Machado, 1998: Fast computation of monochromatic infrared atmospheric transmittances using compressed lookup tables. J. Quant. Spectrosc. Radiat. Transfer, 59, 481-493.

Strow, L.L., D.C Tobin and S.E. Hannon, 1994: A compilation of First-Order Line-Mixing coefficients for CO_2 Q-branches. *J. Quant. Spectrosc. Radiat. Transfer,* **52**, 281.

Strow, L.L., S. E. Hannon, S. De Souza-Machado, H. Motteler and D. Tobin, "An Overview of the AIRS Radiative Transfer Model," IEEE Transactions on GeoSciences and Remote Sensing, 41, 274, 2003.

INTERNATIONAL

ATOVS

WORKING GROUP

Proceedings of the Sixteenth International TOVS Study Conference

Angra dos Reis, Brazil

7-13 May 2008

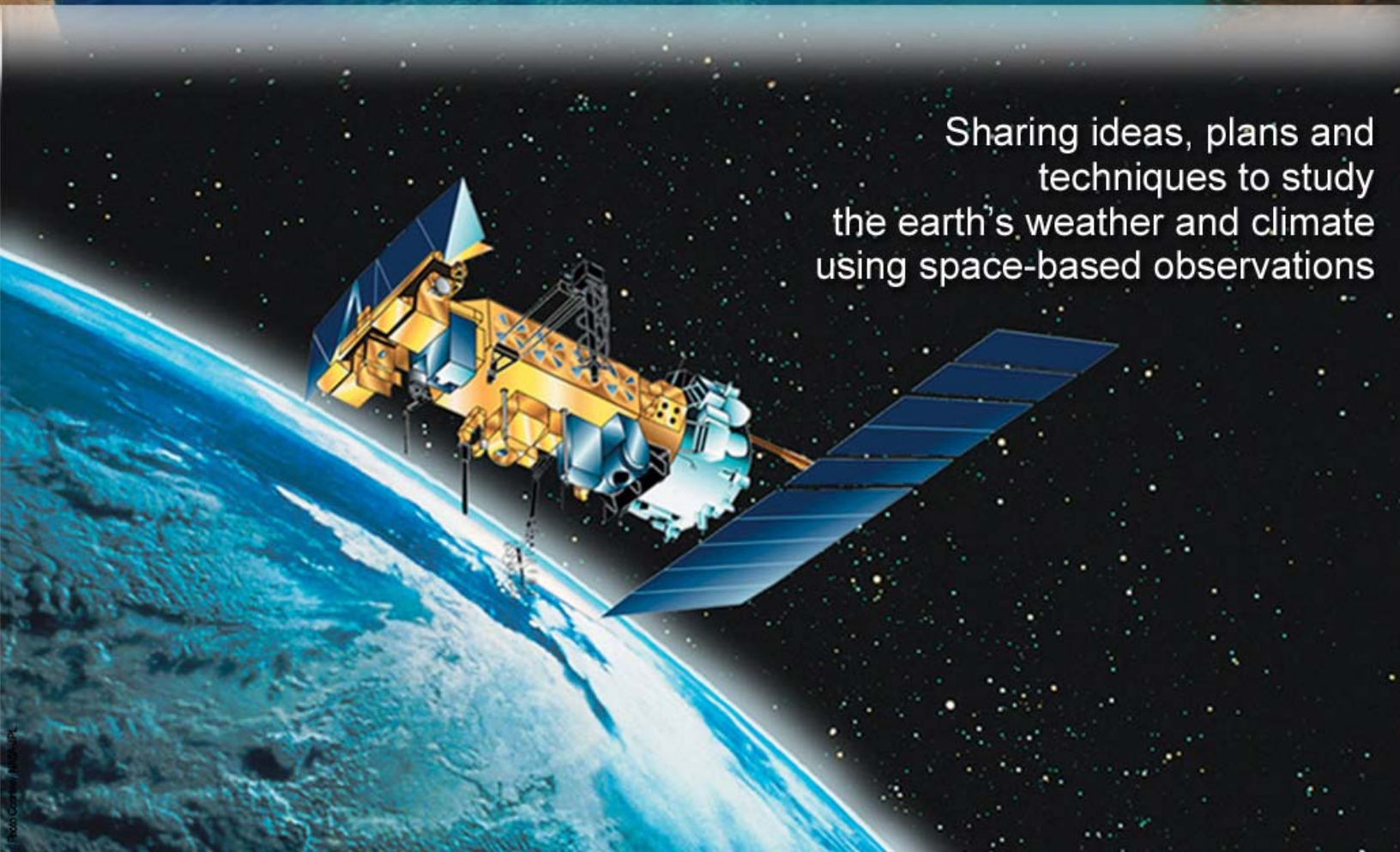

Sharing ideas, plans and techniques to study the earth's weather and climate using space-based observations